# Supporting Information

**Ultrahigh charge–discharge efficiency and high energy density of a high-temperature stable sandwich-structured polymer**

Hanxi Chen[1], Zhongbin Pan[1,2*], Yu Cheng[1], Xiangping Ding[1], Jinjun Liu[1], Qingguo Chi[2], Minhao Yang[3*], Jinhong Yu[4], and Zhi-Min Dang[5*]

[1]School of Materials Science and Chemical Engineering, Ningbo University, Zhejiang, Ningbo 315211, China.

[2]Key Laboratory of Engineering Dielectrics and Its Application, Ministry of Education; School of Electrical & Electronic Engineering, Harbin University of Science and Technology, Harbin 150080, China.

[3]Institute of Advanced Materials, North China Electric Power University, Beijing, 102206, China.

[4]Key Laboratory of Marine Materials and Related Technologies, Zhejiang Key Laboratory of Marine Materials and Protective Technologies, Ningbo Institute of Materials, Technology and Engineering, Chinese Academy of Sciences, University of Chinese Academy of Sciences, Zhejiang, Ningbo 315201, China.

[5]State Key Laboratory of Power System, Department of Electrical Engineering, Tsinghua University, Beijing 100084, China.

***Corresponding author:** panzhongbin@163.com (Zhongbin Pan); ymh0571@163.com (Minhao Yang); dangzm@tsinghua.edu.cn (Zhi-Min Dang)

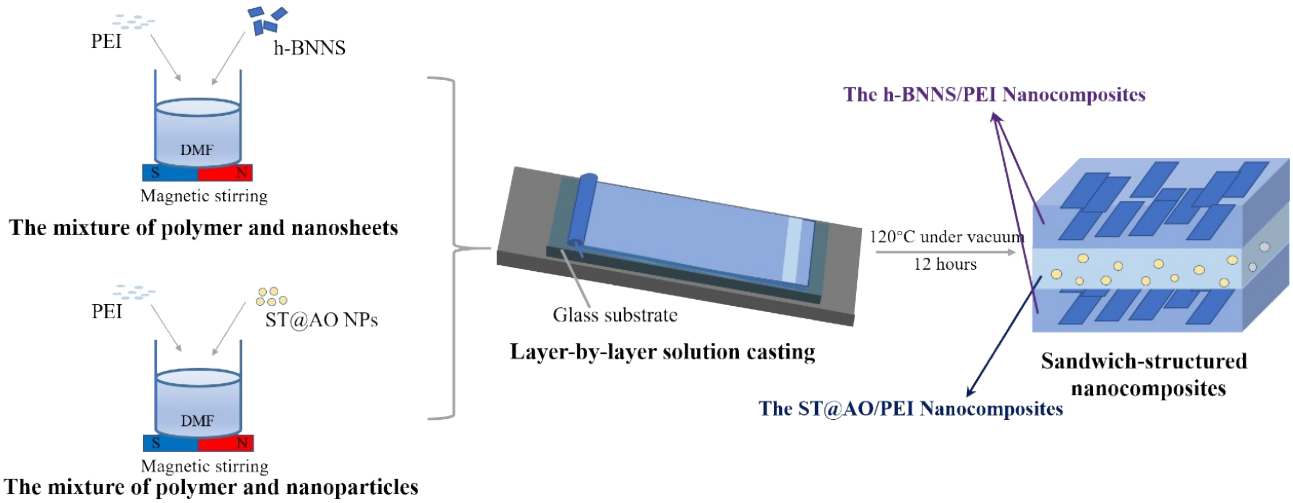


**Fig. S1.** Schematic representation of preparing sandwich-structured film composed of h-BNNS/PEI as outer layers and ST@AO/PEI as the middle layer.

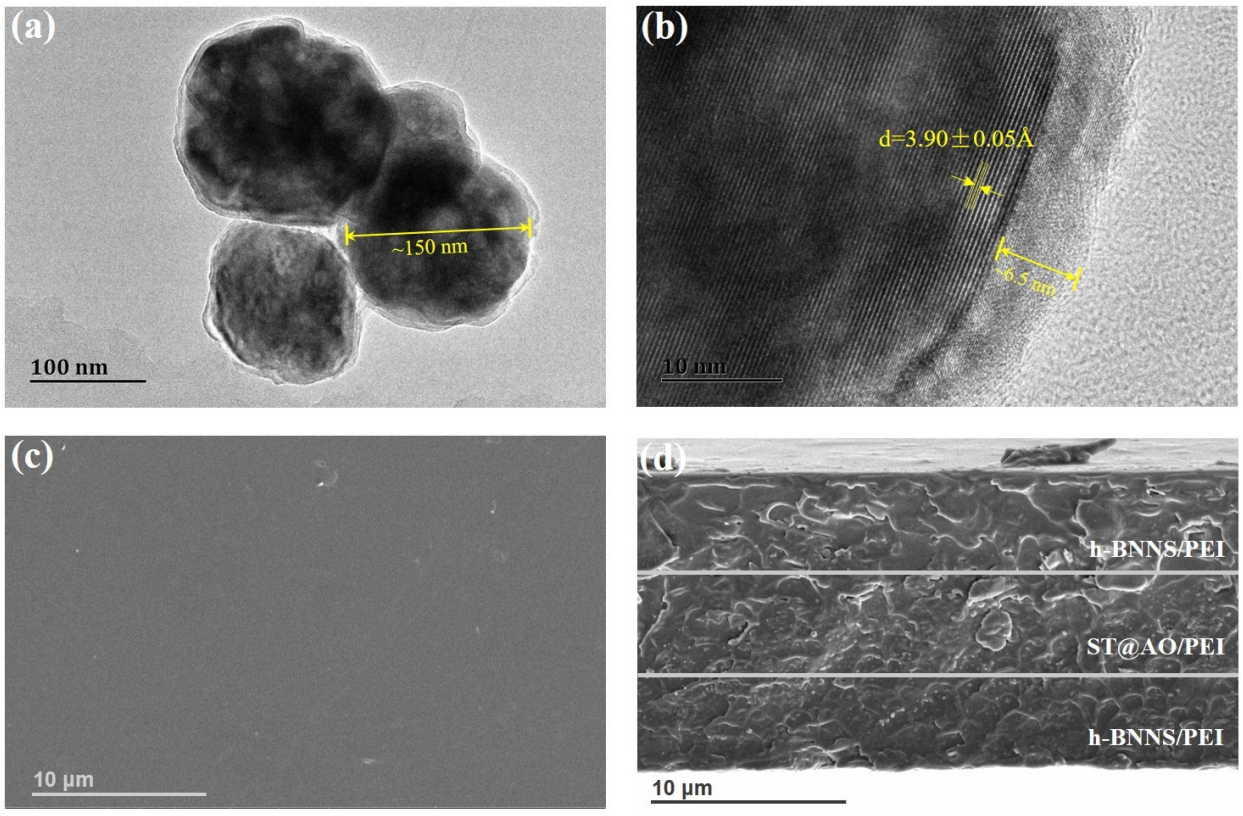


**Fig. S2.** (a) TEM image and (b) HRTEM image of ST@AO NPs. (c) Surface and (d) cross-sectional SEM images of sandwich-structured nanocomposites.

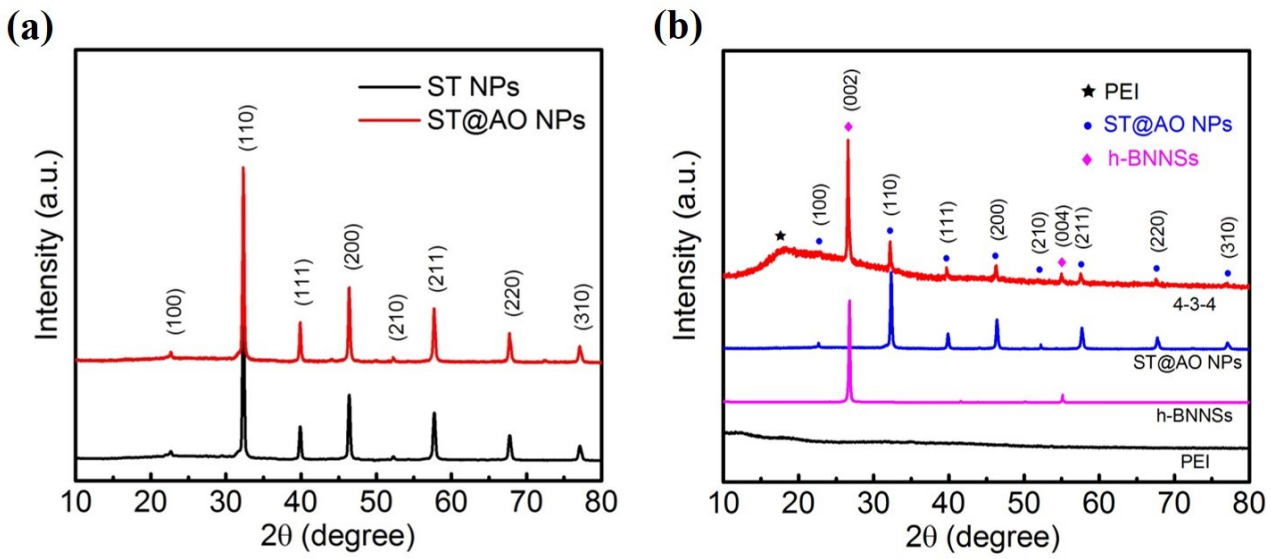


**Fig. S3.** XRD pattern of (a) ST NPs and ST@AO NPs, (b) pure PEI, h-BNNS, ST@AO NPs and sandwich-structured 4-3-4 nanocomposites.

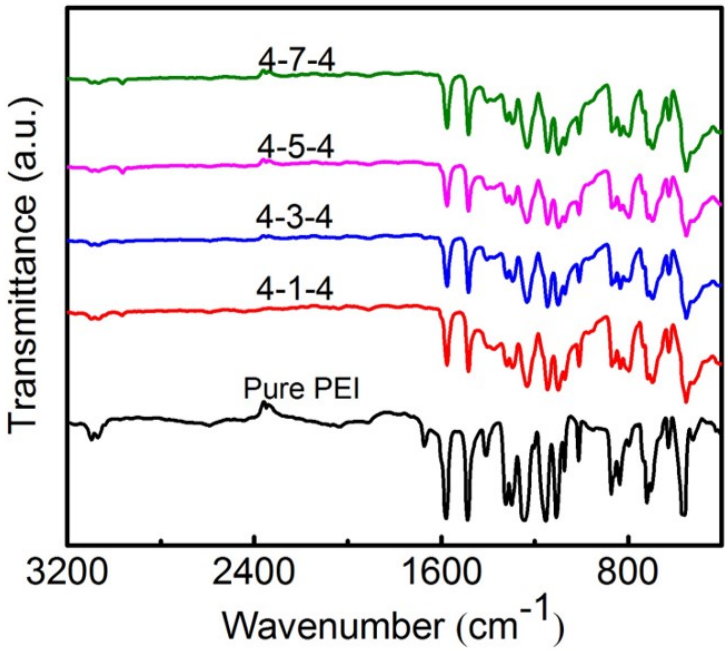


**Fig. S4.** FT-IR spectra of pure PEI and sandwich-structured nanocomposites with different contents of ST@AO NPs in the central layer.

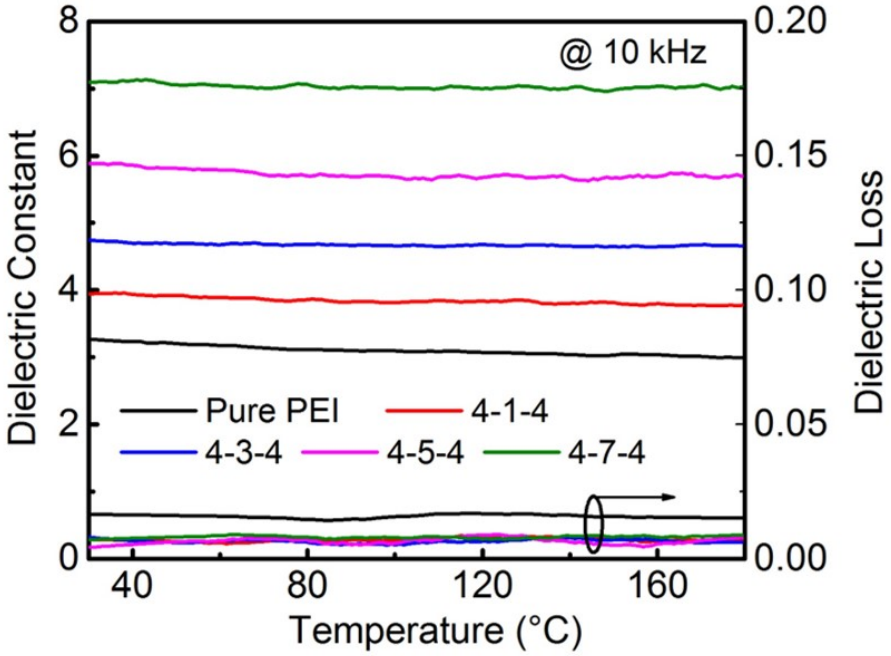


**Fig. S5.** The temperature dependences of dielectric constant and dielectric loss of the pure PEI and all sandwich-structured nanocomposites.

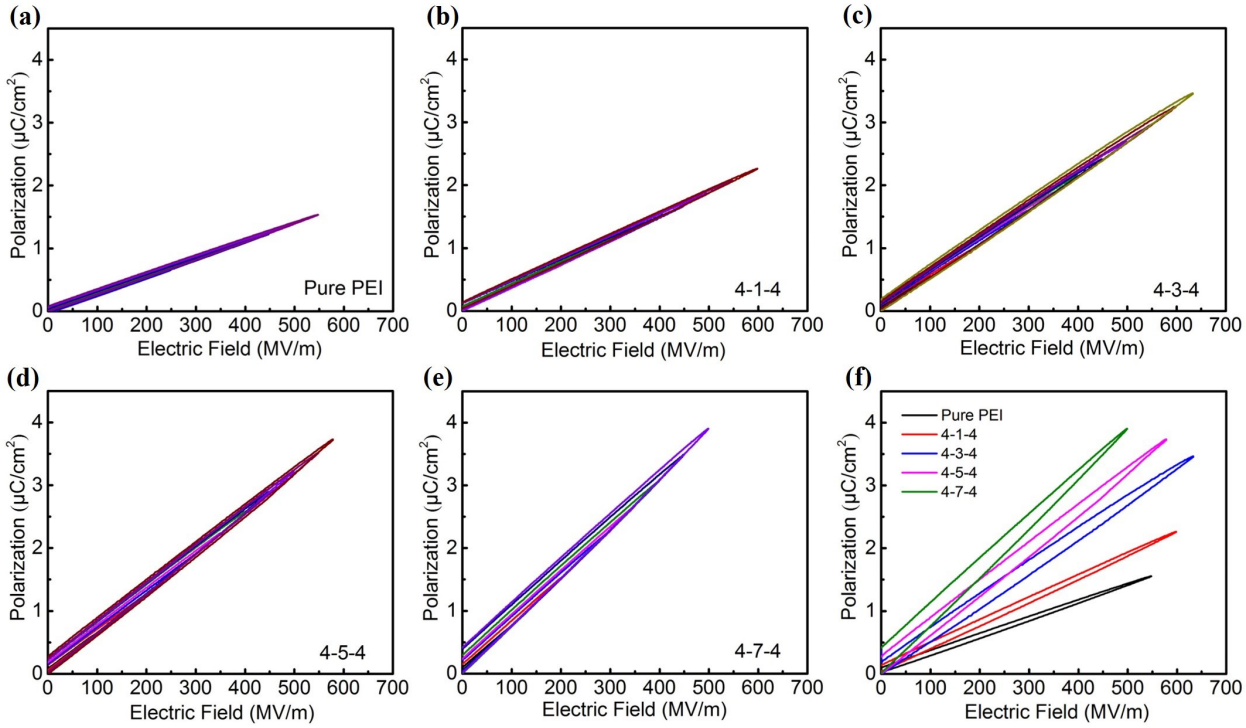


**Fig. S6.** The unipolar *P-E* loops of (a) pure PEI and (b-e) sandwich-structured nanocomposite films with different ST@AO NPs volume fractions in the central layer at varied electric fields at RT. (f) Comparison of the unipolar *P-E* loops near breakdown strength.

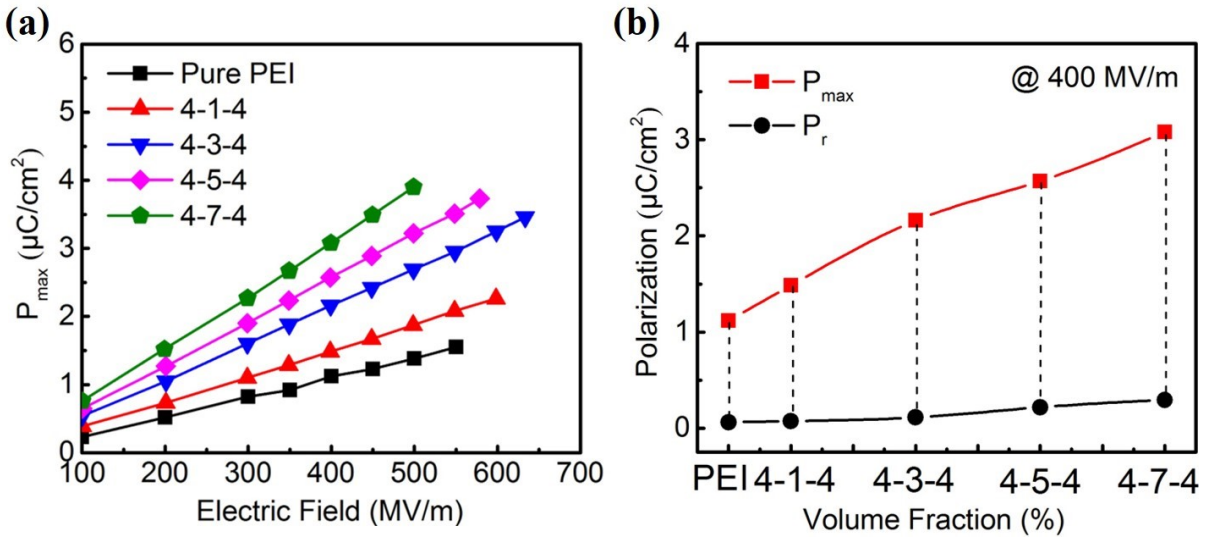


**Fig. S7.** (a) The $P_{max}$ under various electric field and (b) $P_{max}$-$P_r$ at 400 MV/m of pure PEI and sandwich-structured nanocomposite films with different ST@AO NPs contents in the central layer.

\

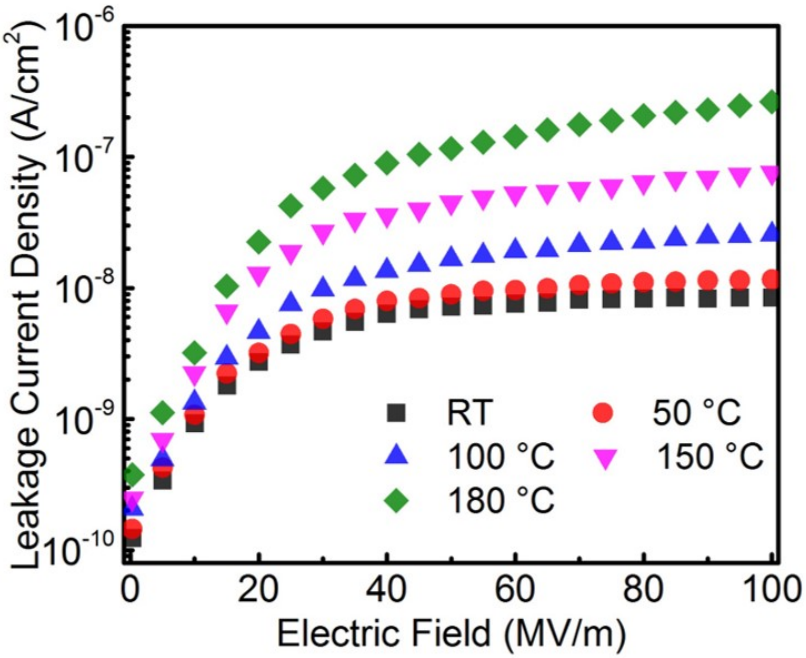


**Fig. S8.** Leakage current density of 4-3-4 nanocomposites at elevated temperature as a function of electric field.

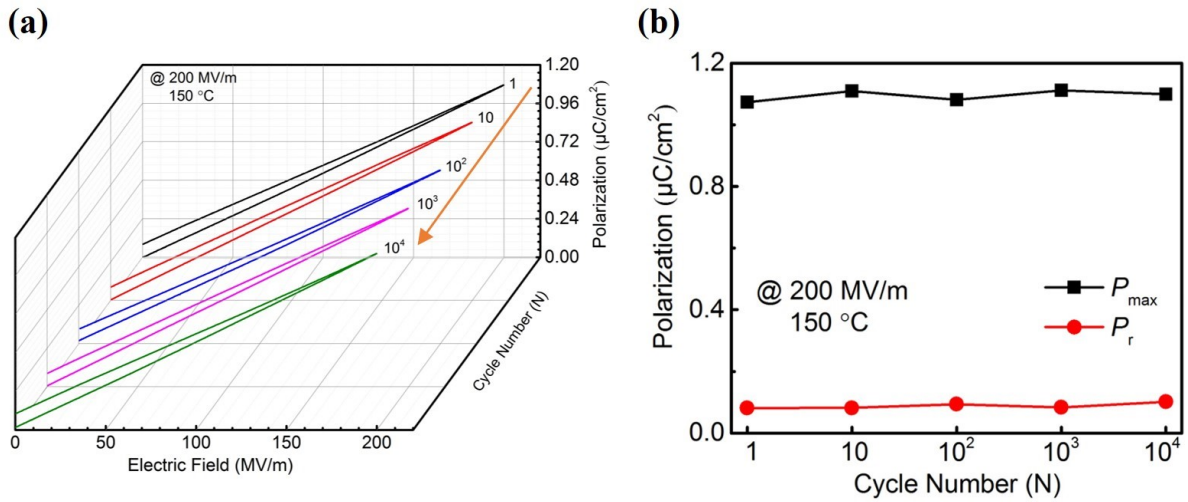


**Fig. S9.** (a) The unipolar *P*-*E* loops, (b) $P_{max}$ and $P_r$ of 4-3-4 (1-10000 cycles at 150 °C and 200 MV/m) as functions of recycles number.

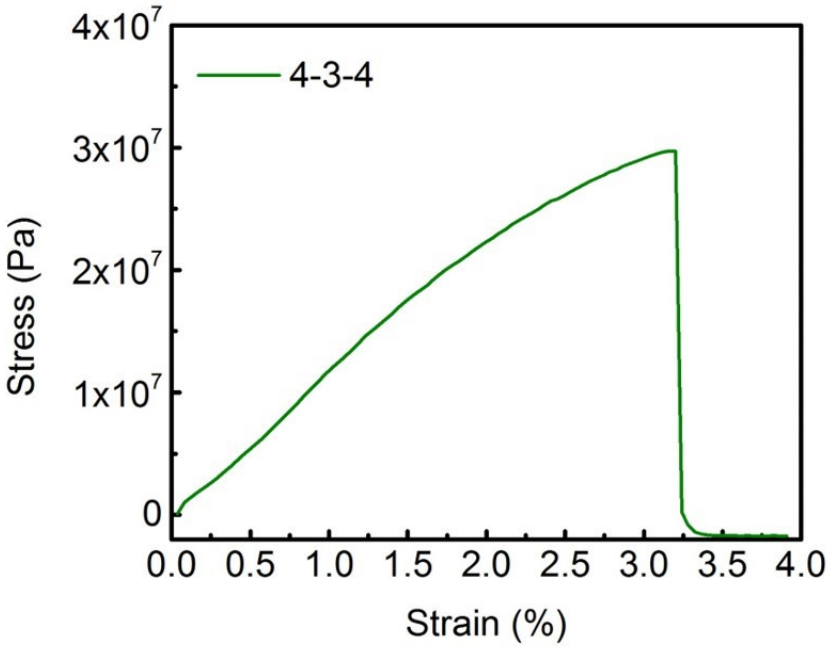


**Fig. S10.** Strain-stress curve of 4-3-4 nanocomposites measured at room temperature.

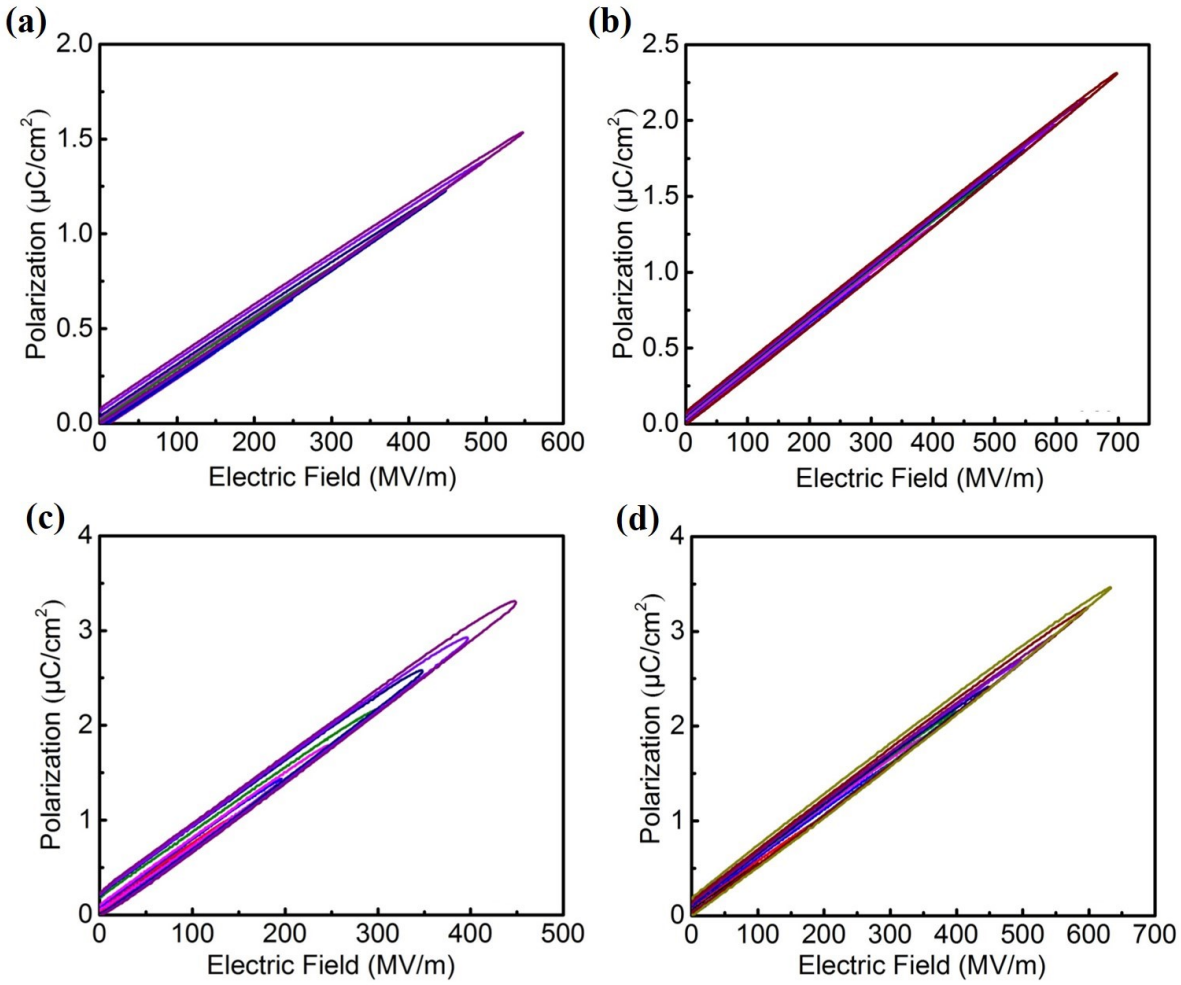


**Fig. S11.** The unipolar *P-E* loops at RT, (a) pure PEI, (b) h-BNNS/PEI, (c) ST@AO/PEI and (d) sandwich-structured 4-3-4 nanocomposite films.

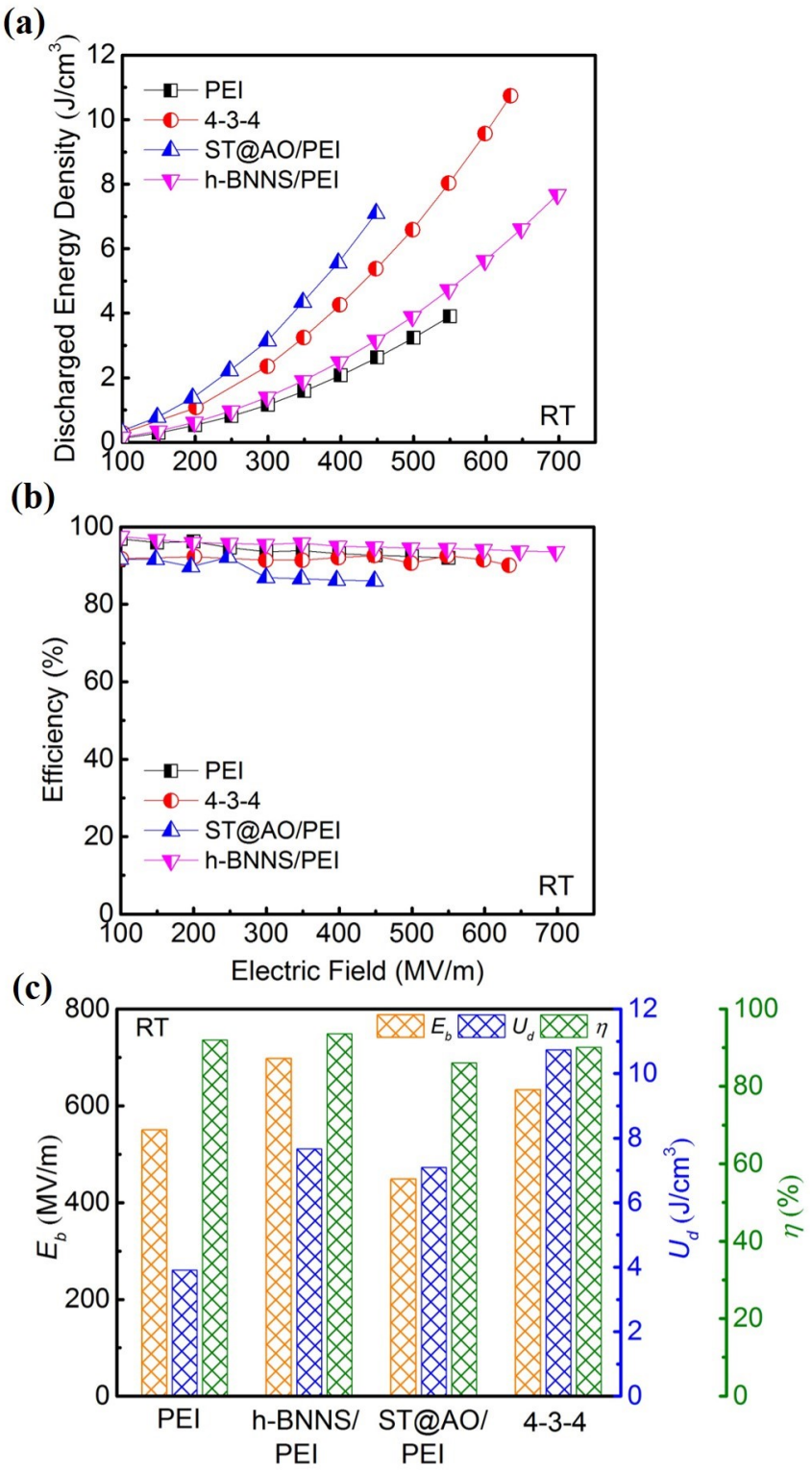


**Fig. S12.** (a) Discharged energy density and (b) efficiency of PEI, h-BNNS/PEI, ST@AO/PEI and 4-3-4 nanocomposites at RT. (c) Summarized of maximum dielectric breakdown strength, discharged energy density and efficiency of PEI, h-BNNS/PEI, ST@AO/PEI and sandwich-structured 4-3-4 nanocomposites at RT.

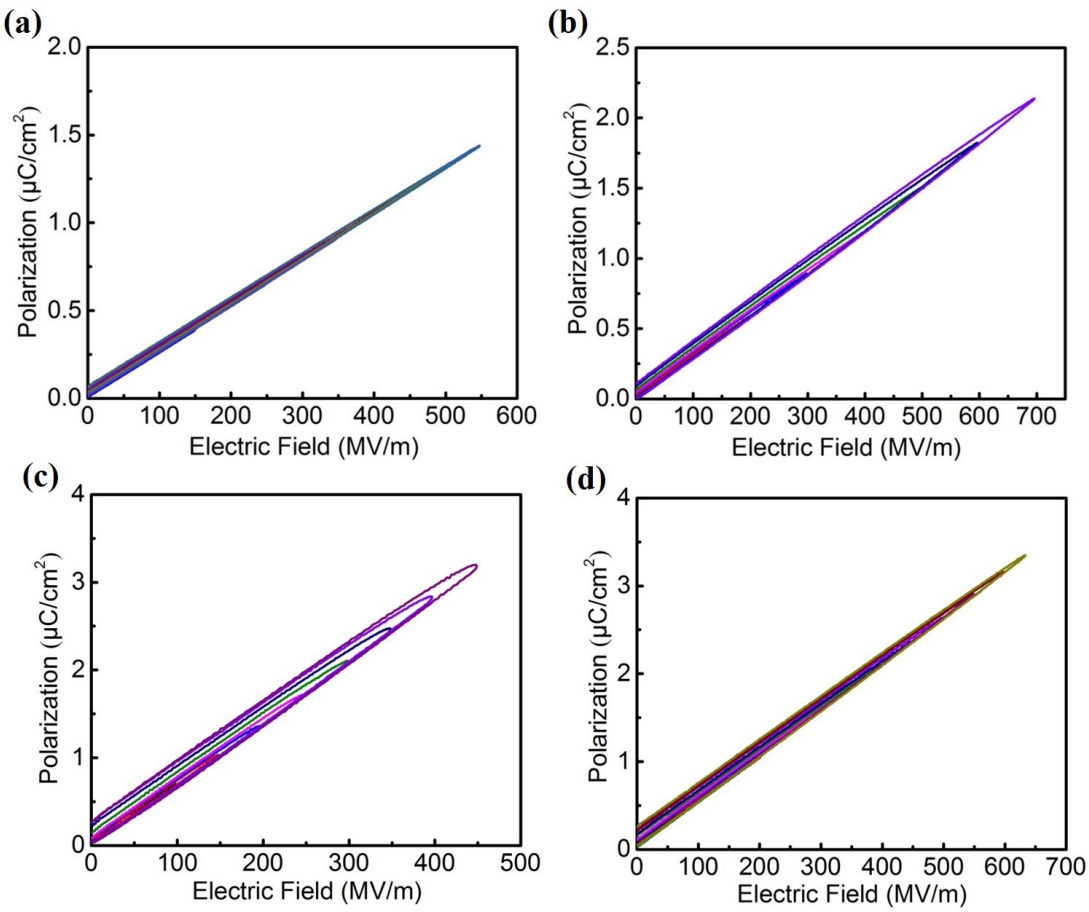


**Fig. S13.** The unipolar *P-E* loops at 50 °C, (a) pure PEI, (b) h-BNNS/PEI, (c) ST@AO/PEI and (d) sandwich-structured 4-3-4 nanocomposite films.

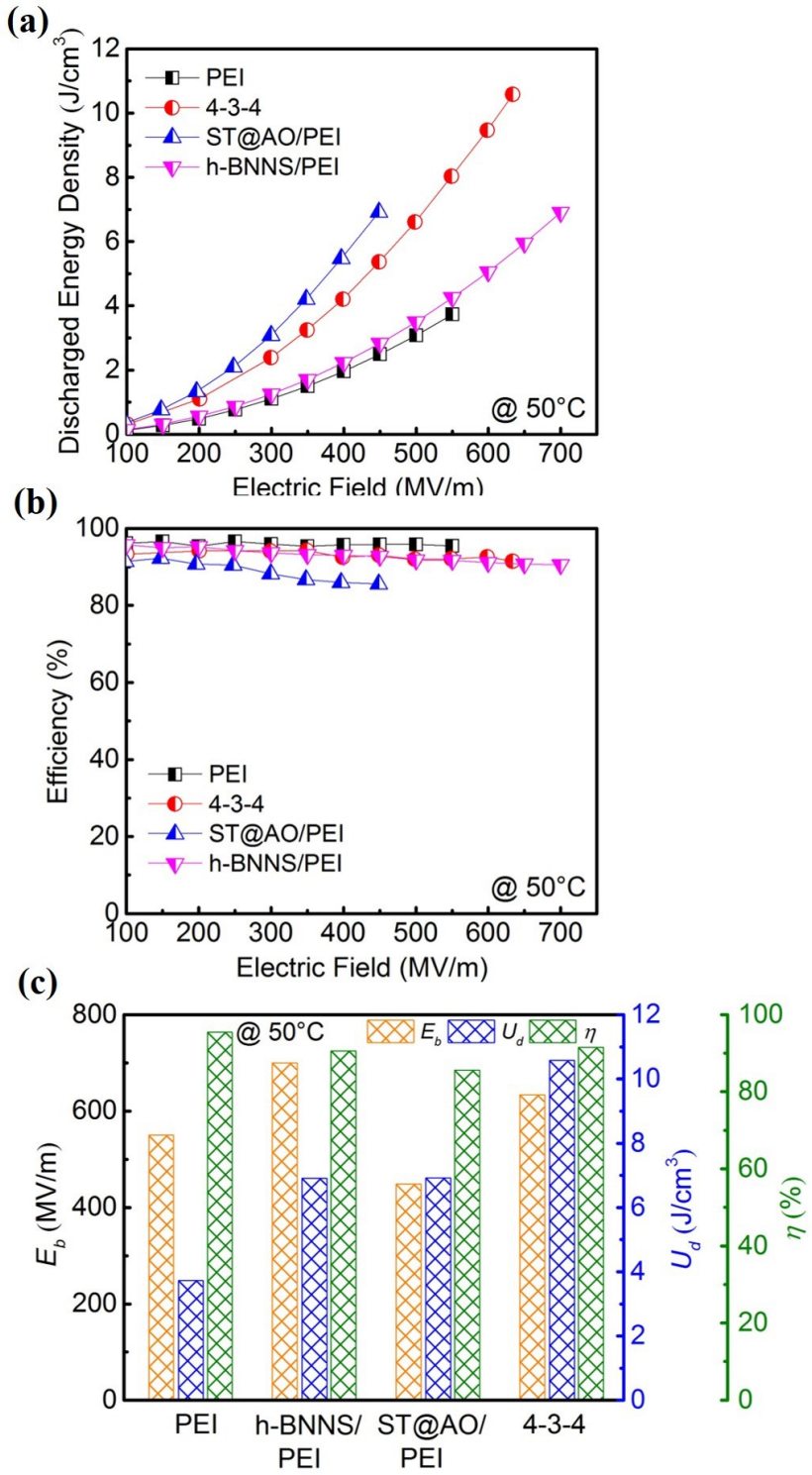


**Fig. S14.** (a) Discharged energy density and (b) efficiency of PEI, h-BNNS/PEI, ST@AO/PEI and 4-3-4 nanocomposites at 50 °C. (c) Summarized of maximum dielectric breakdown strength, discharged energy density and efficiency of the pristine PEI, h-BNNS/PEI, ST@AO/PEI and sandwich-structured 4-3-4 nanocomposites at 50 °C.

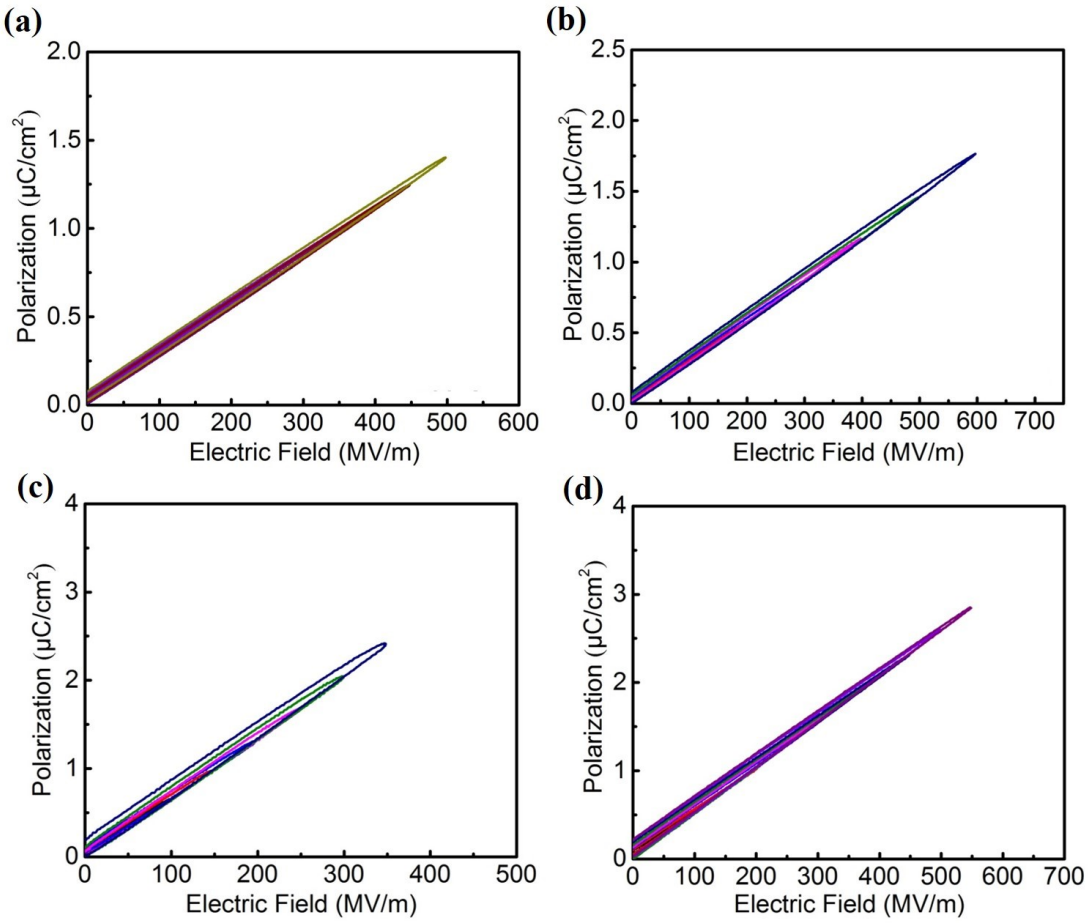


**Fig. S15.** The unipolar *P-E* loops at 100 °C, (a) pure PEI, (b) h-BNNS/PEI, (c) ST@AO/PEI and (d) sandwich-structured 4-3-4 nanocomposite films.

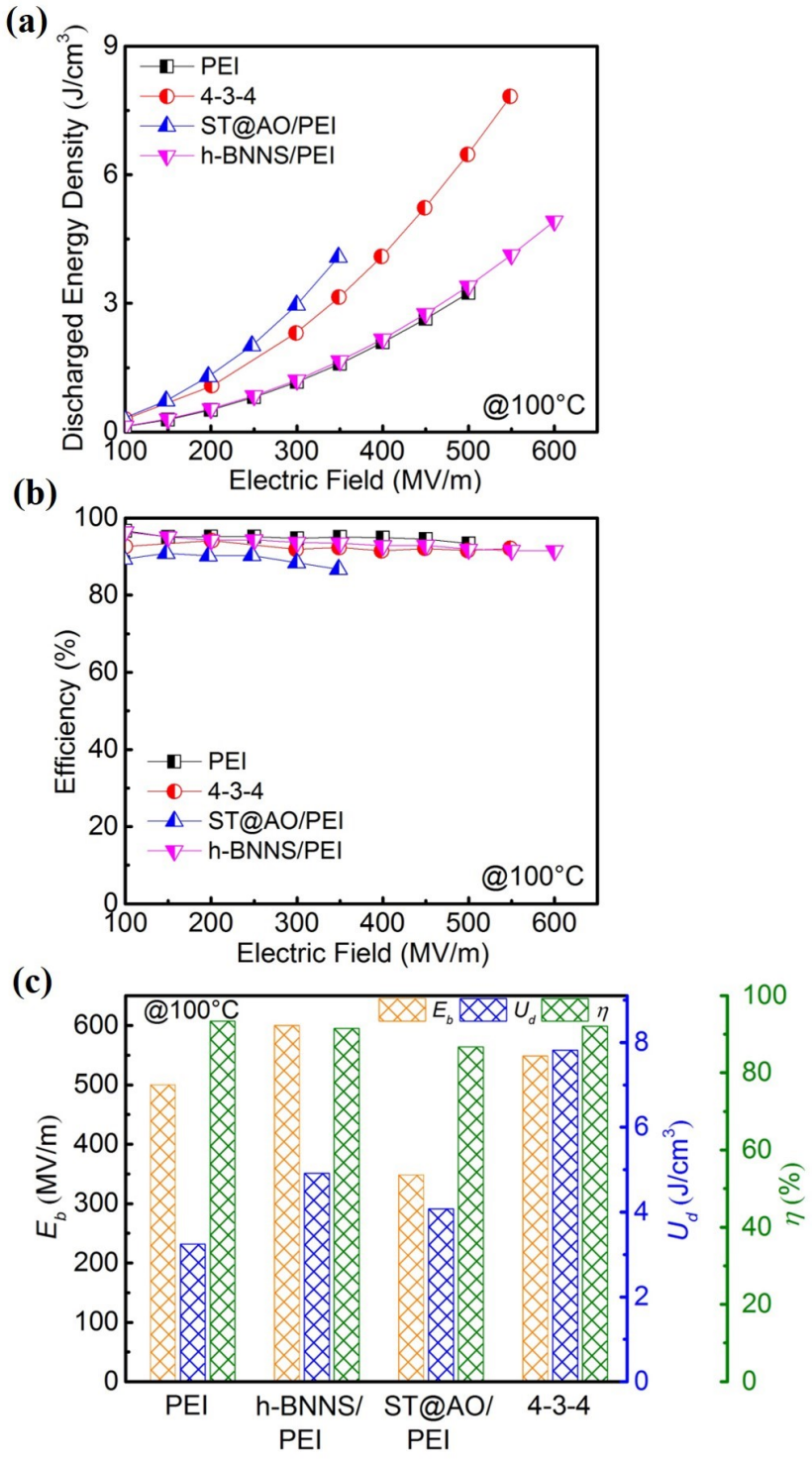


**Fig. S16.** (a) Discharged energy density and (b) efficiency of PEI, h-BNNS/PEI, ST@AO/PEI and 4-3-4 nanocomposites at 100 °C. (c) Summarized of maximum dielectric breakdown strength, discharged energy density and efficiency of the pristine PEI, h-BNNS/PEI, ST@AO/PEI and sandwich-structured 4-3-4 nanocomposites at 100 °C.

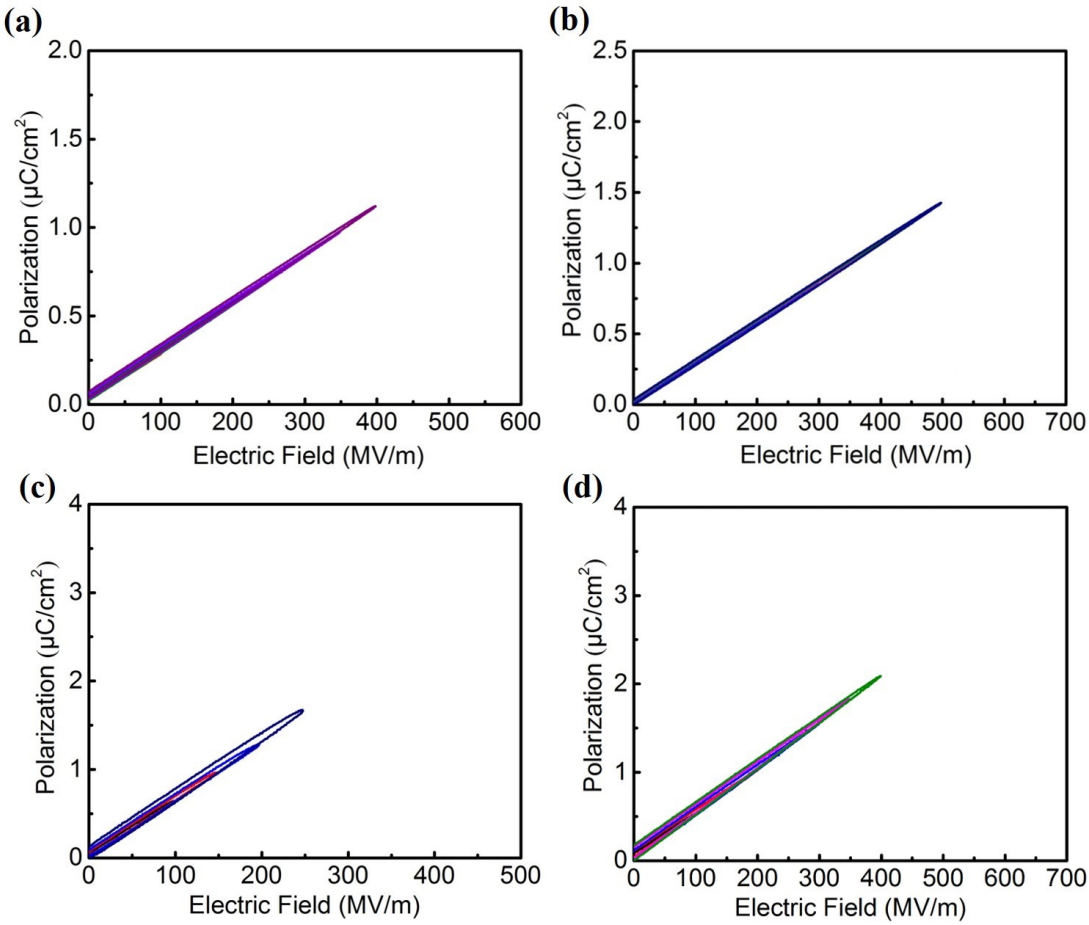


**Fig. S17.** The unipolar *P-E* loops at 150 °C, (a) pure PEI, (b) h-BNNS/PEI, (c) ST@AO/PEI and (d) sandwich-structured 4-3-4 nanocomposite films.

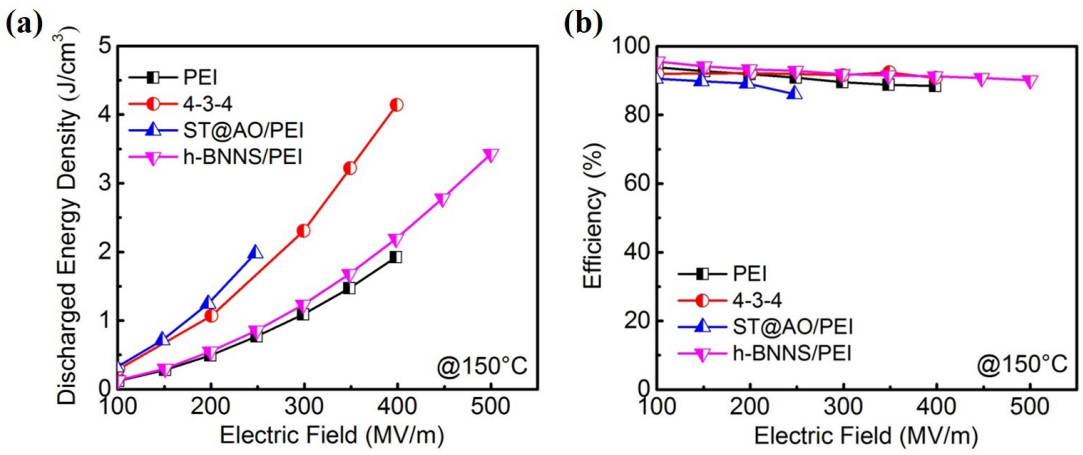


**Fig. S18.** (a) Discharged energy density and (b) efficiency of the pristine PEI, h-BNNS/PEI, ST@AO/PEI and sandwich-structured 4-3-4 nanocomposites at 150 °C.

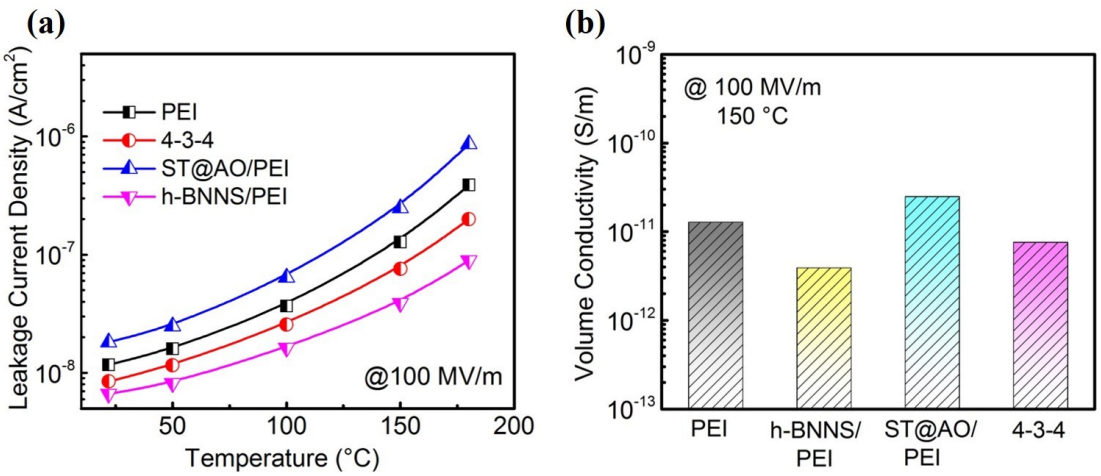


**Fig. S19.** (a) Leakage current density as a function of temperature and (b) volume conductivity under 100 MV/m and 150 °C of single-layer PEI, h-BNNS/PEI, ST@AO/PEI and sandwich-structured 4-3-4 nanocomposites.

**Supporting Information 20**

In this work, the dielectric films with superb flexibility are wound into the actual cylindrical capacitor, on which an aluminum electrode is deposited. The height and radius of the film-wound capacitors are $1.0 \times 10^4$ μm and $5 \times 10^3$ μm, corresponding to the axial and radial direction of the cylindrical capacitor respectively.

For this cylindrical capacitor, the thermal conductivity is considered as two separate values of axial thermal conductivity $K_a$ and radial thermal conductivity $K_r$, respectively, and they can be calculated by the following formula:

$$k_a = k_m V_m + k_{in} V_d$$

$$\frac{1}{k_r} = \frac{V_m}{k_m} + \frac{V_d}{k_{thr}}$$

Where $K_a$ is the thermal conductivity of the cylindrical capacitor electrode layer in the axial direction, and $K_r$ is the radial thermal conductivity of the cylindrical capacitor. $K_m$ is the thermal conductivity of Al electrode, $K_{in}$ and $K_{thr}$ are the thermal conductivity of the composite film along the in-plane and through-plane directions. $V_d$ and $V_m$ are volume fractions of the dielectric film and the metal electrode layer, respectively